Effect of Salt on the Micellization Kinetics of pH-Responsive ABC Triblock Copolymers

Zhiyuan Zhu,[†] Jian Xu,[†] Yueming Zhou,[†] Xiaoze Jiang,[†] Steven P. Armes,[‡] and Shiyong Liu*,[†]

Department of Polymer Science and Engineering, Hefei National Laboratory for Physical Sciences at the Microscale, University of Science and Technology of China, Hefei, Anhui 230026, China, and Department of Chemistry, University of Sheffield, Brook Hill, Sheffield, South Yorkshire S37HF, United Kingdom

Received April 27, 2007; Revised Manuscript Received June 26, 2007

ABSTRACT: The pH-induced micellization kinetics of poly(glycerol monomethacrylate)-*b*-poly(2-(dimethylamino)ethyl methacrylate)-*b*-poly(2-(diethylamino)ethyl methacrylate) (PGMA-*b*-PDMA-*b*-PDEA) in the presence of salt (NaCl) was investigated by stopped-flow light scattering and fluorescence, and the results were compared to those obtained with salt-free solutions. Upon jumping from pH 4 to 12, this triblock copolymer forms micelles that consist of a central PDEA core, shielded by a PDMA inner shell and a PGMA outer corona. For micelle formation in the presence or absence of salt, all relaxation curves recorded by stopped-flow light scattering can be well fitted with a double-exponential function, leading to a fast relaxation time constant (τ_1) and a slow relaxation time constant (τ_2). The fast process (τ_1) is associated with the formation of quasi-equilibrium micelles, while the slow process (τ_2) is associated with micelle formation−breakup, approaching the final equilibrium state. Both processes occur much more slowly on initial addition of NaCl and then level off at higher salt concentrations (>0.5 M NaCl). The concentration dependence of τ_2 revealed that the mechanism of micelle formation/breakup process transforms from unimer insertion/expulsion in the absence of salt to micelle fusion/fission in the presence of high NaCl concentrations. This is because the PGMA corona and PDMA inner are less highly hydrated and the PDEA core is more compact in the presence of salt, thus favoring micelle fusion/fission instead of unimer insertion/expulsion. Relaxation curves obtained with stopped-flow fluorescence using pyrene as a probe can be well-fitted with a single-exponential function, and the relaxation time (τ_{py}) was in agreement with τ_f, the relaxation time of the overall micellization process as detected by stopped-flow light scattering. Compared to the kinetics obtained with salt-free solutions, the micelle dissociation kinetics in the presence of salt resulting from a pH jump from 12 to 4 reveals a drastically different two-stage process with the two stages separated by a delay time of a few seconds.

Introduction

In selective solvents, amphiphilic block copolymers can self-assemble into micelles and mesophases of various morphologies.[1−6] Among them, stimuli-responsive double hydrophilic block copolymers (DHBCs) represent a special case. They exhibit so-called "schizophrenic" micellization behavior in aqueous solution upon a judicious combination of external stimuli, such as pH, ionic strength, and temperature.[7−22] Past studies of DHBCs mainly focused on the characterization of their equilibrium self-assembled nanostructures, whereas a molecular-level understanding of the mechanism and kinetics of micellization has remained unexplored.

The micellization dynamics of small molecule surfactant near the association equilibrium can be relatively well described by the Aniansson and Wall (A−W) theory.[23−25] An important assumption in the A−W theory is that all changes are due to an elementary process of insertion/expulsion of individual chains ("unimers") into/out of the micelle. This interpretation has been confirmed by many experiments using classical relaxation techniques such as stopped-flow, temperature-jump, pressure-jump, and ultrasonic absorption. However, micelle formation/dissociation may also involve a fusion/fission mechanism, especially at higher copolymer concentrations or in the presence of salt.[26,27] Winnik et al.[28] studied the exchange mechanisms for sodium dodecyl sulfate (SDS) micelles in the presence of NaCl using a highly hydrophobic pyrene probe. Their results indicated two micelle fusion/fission mechanisms, fission growth and collision-exchange fission, depending on the salt concentration.

Like small molecule surfactants, the micellization kinetics of block copolymers is also closely related to their stability, which plays an important role in various technological processes such as foaming, wetting, emulsification, solubilization, and detergency.[29,30] On the basis of A−W theory, now generally accepted for the micellization behavior of small molecule surfactants, Halperin and Alexander examined the relaxation kinetics of block copolymer micelles when subjected to small perturbations.[31] They proposed that the insertion/expulsion mechanism is the only mechanism that is relevant for block copolymers, i.e., that unimer expulsion is the rate-determining step in copolymer micelle formation and dissociation.

Mattice et al.[32] performed computer simulations for large deviations from the initial state, such as a unimer−micelle transition. This study suggested the presence of two processes with different time scales, the volume fraction of free chains reached its equilibrium value very quickly in the fast step, followed by a slower step toward the equilibrium state. Dormidontova and co-workers further proposed a micelle fusion/fission−unimer expulsion/entry joint mechanism for block copolymer micelle growth, suggesting that micelle fusion/fission

* To whom correspondence should be addressed. E-mail: sliu@ustc.edu.cn.
[†] University of Science and Technology of China.
[‡] University of Sheffield.

10.1021/ma070978h CCC: $37.00
Published on Web 07/31/2007

dominates over unimer entry/expulsion in the initial (fast) process, while unimer entry/expulsion mechanism dominates during the second (slower) process.[33] However, Semenov et al.[34,35] recently postulated that the unimer−micelle transition cannot be simply characterized by just two relaxation times, but rather by a continuous spectrum of relaxation times. These workers also proposed that the main route to micelle formation should involve step-by-step addition of unimers, i.e., the insertion/expulsion of individual chains.[34] Thus, a theoretical consensus regarding the detailed formation and dissociation mechanism(s) of block copolymer micelles has not yet been established.

Experimental studies of block copolymer micellization kinetics are rare. Honda et al.[36,37] and Iyama et al.[38,39] studied the kinetics of block copolymer micellization in organic solvents using static and dynamic laser light scattering (LLS). They interpreted their micellization kinetics in terms of the A−W theory, although a large deviation from the equilibrium state was involved. In the fast process, rapid unimer association resulted in the formation of quasi-equilibrium micelles, and an increase in number density of these quasi-equilibrium micelles dominated over the growth of larger micelles. Micelle growth and partial decomposition of the quasi-equilibrium micelles were involved in the subsequent slower process, approaching the final equilibrium state. Structural evolution during the unimer−micelle transition could not be discounted. The limitation of time-resolved static and dynamic LLS is that it needs a relatively long thermal equilibration period, so the kinetic details of the early stages could not be probed.

Previously, we reported the kinetics of pH-induced micellization of a pH-responsive ABC triblock copolymer, namely poly(glycerol monomethacrylate)-*b*-poly(2-(dimethylamino)ethyl methacrylate)-*b*-poly(2-(diethylamino)ethyl methacrylate) (PGMA-*b*-PDMA-*b*-PDEA), using stopped-flow light scattering.[40] Upon jumping from pH 4 to 12, the early stages of micellization occurred via two successive processes. The first fast process (τ_1) is associated with the formation of quasi-equilibrium micelles, and the second slow process (τ_2) is associated with micelle formation and breakup, approaching the final equilibrium state. The characteristic time constant τ_2 is almost independent of the copolymer concentration, indicating that the slow process proceeds mainly via the unimer insertion/expulsion mechanism.

It should be noted that the practical applications of block copolymer micelles usually involve additives such as salt. The nature of this added salt and its concentration can exert a marked influence on the aqueous solubility of water-soluble polymers and consequently the aggregation behavior of block copolymers.[41−44] To become hydrated, the added salt must compete with the hydrophilic polymer chains for the water molecules. Tam et al.[41] recently reported subtle salt effects on the self-assembly behavior of a 4-arm star block copolymer and showed that the presence of a small amount of salt can significantly affect the micelle structures. Both Peyrelasse et al.[43] and Bahadur et al.[42] reported that addition of NaCl to aqueous solutions of PEO−PPO−PEO copolymers produces a "salting out" effect, favoring the formation of micelles with more compact cores.

Herein, we further investigated the effect of salt addition on the pH-induced unimer−micelle transition kinetics of PGMA-*b*-PDMA-*b*-PDEA in aqueous solution using a pH-jump stopped-flow technique. This triblock copolymer dissolved molecularly in aqueous solution below pH 6; upon addition of base, micellization occurred above pH 7 to form three-layer "onion-like" micelles consisting of PDEA cores, solvated PDMA inner shells, and PGMA outer coronas. To explore the effect of the extent of dehydration of the core and coronal chains on the micellization dynamics, the mechanism of the slow process, micelle formation−breakup, was compared to that obtained with salt-free solutions. Using a pyrene probe, stopped-flow fluorescence was also employed to detect the properties of intermediates formed during micellization.

Experimental Section

Materials. Glycerol monomethacrylate (GMA) was kindly donated by Cognis Performance Chemicals (UK). 2-(Dimethylamino)ethyl methacrylate (DMA) and 2-(diethylamino)ethyl methacrylate (DEA) were obtained from Aldrich. Each monomer was passed through its own basic alumina column, then vacuum-distilled from CaH_2, and stored at −20 °C prior to use. Triethylamine (TEA) was dried over CaH_2 and distilled at reduced pressure. Copper(I) bromide (CuBr, 98%, Aldrich), 2,2′-bipyridine (bpy, 99+%, Aldrich), 2-bromoisobutyryl bromide (98%, Aldrich), pyrene (98%, Aldrich), monohydroxy-capped poly(ethylene glycol) with a mean degree of polymerization (DP) of ∼6−7 (designated OEG-OH, Cognis), and all other chemicals were used as received.

The triblock copolymer, PGMA-*b*-PDMA-*b*-PDEA, was synthesized via atom transfer radical polymerization (ATRP) using sequential monomer addition, as described previously.[40] The M_n of the triblock copolymer determined by GPC relative to polystyrene standards was ∼35 000 g mol^{-1}, with an M_w/M_n of 1.25. The mean DP values of the PGMA, PDMA, and PDEA blocks were calculated to be 45, 34, and 52, respectively, from an ^{1}H NMR spectrum recorded in CD_3OD using the OEG-OH initiator fragment as a convenient end group.

Laser Light Scattering (LLS). Measurements were conducted using a commercial spectrometer (ALV/DLS/SLS-5022F) equipped with a multitau digital time correlation (ALV5000) and a cylindrical 22 mW UNIPHASE He−Ne laser ($\lambda_0 = 632$ nm) as the light source. The correlation functions were analyzed by the cumulant method and CONTIN software. Distribution averages and particle size distributions were computed using cumulants analysis and CONTIN routines. Scattered light was detected over scattering angles ranging from 45° to 90°. The angular dependence of the quantity Γ/q^2, where Γ is the decay rate of the correlation function and q is the scattering vector, was negligible for all the micellar solutions. Thus, the intensity-average hydrodynamic radius, $\langle R_h \rangle$, at a scattering angle of 90° were reported. It has been previously shown that the scattering contribution from small ions becomes significant only in very concentrated salt solutions, e.g., in 3−4 M NaCl solutions.[45] Thus, this contribution is negligible in the current study. The solution pH was adjusted as required using concentrated NaOH or HCl. Dust particles were removed by filtering the copolymer solutions through 0.45 μm pore-size membrane filters (Millipore).

Stopped-Flow Kinetic Study. Stopped-flow studies were carried out using a Bio-Logic SFM300/S stopped-flow instrument. The SFM-3/S is a three-syringe (10 mL) instrument in which all step-motor-driven syringes (S1, S2, and S3) can be operated independently for either single- or double-mixing. The SFM-300/S stopped-flow device is attached to the MOS-250 spectrometer; kinetic data were fitted using the program Biokine (Bio-Logic). For light scattering detection at 90°, both the excitation and emission wavelengths were adjusted to 335 nm with 10 nm slits. For fluorescence detection, excitation and emission wavelength was adjusted to 330 and 370 nm with 5 nm slits, respectively. Using FC-08 or FC-15 flow cells, the typical dead times are 1.1 and 2.6 ms, respectively.

For the stopped-flow fluorescence measurements, pyrene was added to all copolymer solutions. A known volume of pyrene in acetone (0.1 mL, 1.0 mM) was first introduced into a 100 mL volumetric flask, and acetone was evaporated under a stream of nitrogen flow. An aqueous solution containing the triblock copolymer or NaOH with various NaCl concentrations was then added, and the final pyrene concentration was fixed at 1×10^{-6} M. The

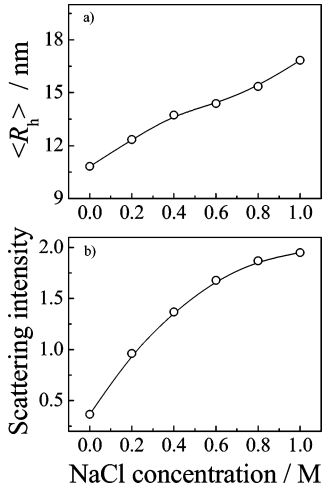

Figure 1. Variation of (a) average hydrodynamic radius, $\langle R_h \rangle$, at a scattering angle of 90° and (b) scattering light intensities at a scattering angle of 15° obtained for 1.0 g/L aqueous solution of PGMA-*b*-PDMA-*b*-PDEA micelles formed at pH 12 as a function of added NaCl.

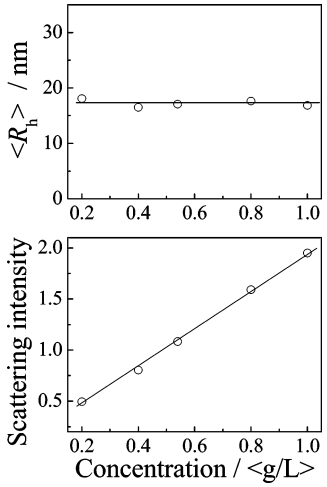

Figure 2. Variation of hydrodynamic radius, $\langle R_h \rangle$, and scattering light intensities as a function of copolymer concentration at pH 12 in the presence of 1.0 M NaCl.

pyrene-containing copolymer solution was sonicated for 20 min and then slowly stirred overnight.

Results and Discussion

LLS Studies. The micellization behavior of this PGMA-*b*-PDMA-*b*-PDEA triblock copolymer in *salt-free* solutions were investigated previously.[40] PDEA homopolymer is water-insoluble at neutral or alkaline pH. Below pH 6, it is soluble as a weak cationic polyelectrolyte due to protonation of its tertiary amine groups. Thus, this triblock copolymer is molecularly dissolved below pH 6−7. On addition of NaOH, micellization occurred above pH 7.3, as indicated by the bluish tinge that is characteristic of micellar solutions.[40] The formed micelles are expected to have a three-layer "onion" structure, with the PDEA block occupying the micelle cores and the PDMA and PGMA blocks forming the inner shells and coronas, respectively.

Typically, the effect of added electrolytes on the micellization properties of nonionic block polymers is not as remarkable as that observed for block polyelectrolytes, where counterion condensation onto the charged micelle surface drastically screens corona chain repulsion. Peyrelasse et al.[43] and Bahadur et al.[42] reported that NaCl addition in aqueous solution of Pluronics produces a "salting out" effect. Upon salt addition, both PEO and PPO blocks became dehydrated to a similar extent, whereas the effect on the solubility of the PPO blocks is rather more pronounced, resulting in a lowering of the critical micellization temperature (CMT) and favoring the formation of micelles with more compact cores.[44] Thus, the micellar self-assembly of Pluronics can be induced by either increasing the temperature or adding NaCl. In both cases the unimer chains become progressively more dehydrated. Kositza et al.[46] studied the salt-induced micellization kinetics of Pluronic L64 at room temperature.

Figure 1 shows the dynamic LLS data obtained for the triblock copolymer at pH 12 in the presence of various NaCl concentrations. The intensity-average hydrodynamic radius, $\langle R_h \rangle$, at a scattering angle of 90°, gradually increased from 11 to 17 nm when the NaCl concentration was increased from 0 to 1.0 M (Figure 1a). This indicates that the added salt exerts a "salting out" effect on the PGMA, PDMA, and PDEA blocks. It should be noted that all three blocks are neutral at pH 12. The reduced hydrophilic character of the PGMA and PDMA blocks should favor larger micelles.

From Figure 1b, the scattering light intensities at a scattering angle of 15° increase more abruptly than that of $\langle R_h \rangle$ with the initial increase in ionic strength. A rough calculation indicated that upon increasing the NaCl concentration from 0 to 1.0 M the hydrodynamic volume of block copolymer micelles increased ~3.8 times, while the scattering intensities increased ~5.3 times. It should be noted that, at low scattering angles (15°), the scattering intensities should be more closely related to the average molar mass, $M_{w,app}$, of the micelles. Thus, the micelle density increases with the addition of salt; i.e., the micelles are becoming more compact. The shrinking PGMA and PDMA chains and denser packing of PDEA chains in the micelle cores should both contribute to the above conformational changes.

Figure 2 shows the dynamic LLS results of the triblock copolymer micelles formed at different copolymer concentrations in the presence of 1.0 M NaCl. The $\langle R_h \rangle$ of the micelles remains nearly unchanged as the copolymer concentration ranges from 0.2 to 1.0 g/L. Moreover, the light scattering intensities of the micellar solution monotonically increase with copolymer concentration. This indicates that increasing the copolymer concentration does not affect the micelle size and micelle density (compactness); only the number-density of micelles increases with copolymer concentration.

Stopped-Flow Kinetics Studies. *Final Salt Concentration Dependence of Micellization Kinetics.* The double mixing setup of the stopped-flow apparatus is convenient for either pH jump or salt jump experiments or a combination of the two. Figure 3 shows a typical dynamic curve recorded during micelle formation induced by a pH jump from 4 to 12 in the presence of 1.0 M NaCl: only one relaxation process with a quite large positive amplitude can be observed. The time dependence of the scattered light intensity I_t can be converted to a normalized function, namely, $(I_\infty - I_t)/I_\infty$ vs t, where I_∞ is the value of I_t at an infinitely long time. Single- and double-exponential fitting results are also shown in Figure 3. The quality of the fit is assessed from the reduced χ^2 error values, which is defined by

$$\chi^2 = \frac{1}{N}\sum_{i=1}^{N}(x_i - \bar{x}_i)^2 \qquad (1)$$

where N, x_i, and $\bar{x}_i$ are the number of data points and the values of the experimental data and the fitting data, respectively.

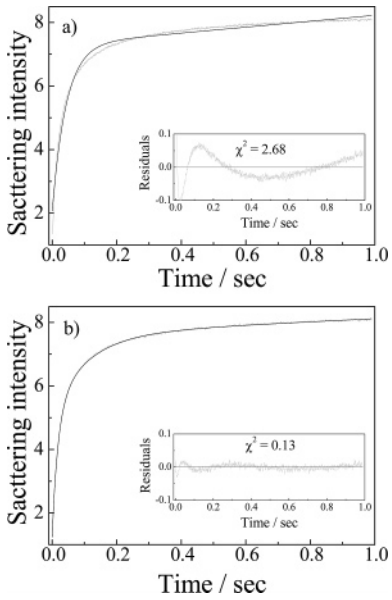

Figure 3. Typical time dependence for the scattering light intensity recorded during micellization induced by a pH jump from 4 to 12 in the presence of 1.0 M NaCl. The upper and lower figures are fitted by (a) single- and (b) double-exponential functions, respectively. The final copolymer concentration is fixed at 1.0 g/L.

It was found that single-exponential function cannot fit the relaxation curve very well (Figure 3a), especially for the first 0.2 s. The reduced χ^2 error value for the single-exponential fitting is 2.68. However, the kinetic trace could be well-fitted by a double-exponential function (Figure 3b, eq 2), leading to a prominent improvement of χ^2 to 0.13.

$$\frac{I_t - I_\infty}{I_\infty} = c_1 e^{-t/\tau_1} + c_2 e^{-t/\tau_2} \tag{2}$$

where c_1 and c_2 are the normalized amplitudes, and $c_2 = 1 - c_1$, τ_1, and τ_2 are the characteristic relaxation times for the two processes, such that $\tau_1 < \tau_2$. The relaxation time for the overall micellization process, τ_f, can be calculated as

$$\tau_f = c_1\tau_1 + c_2\tau_2 \tag{3}$$

The fitting of relaxation curves to monitor micelle formation in the presence of salt was similar to that in the absence of salt, as reported previously.[40] The calculated relaxation time constants, τ_1 and τ_2, are ascribed to two successive processes. The fast relaxation process (τ_1) is associated with the rapid association of unimers to form quasi-equilibrium micelles, while the slow process (τ_2) is associated with the micelle formation−breakup process on approaching the final equilibrium state. This final equilibrium state has not been attained within the time window of our experiments. Even after 10 min, the light scattering intensity from the micelles is still increasing slightly.

In the current study, we focused solely on the early stages of the micelle formation process, during which the most dramatic changes occur. On longer time scales, we believe that the relaxation of the unimer−micelle transition into the final equilibrium state should follow equilibrium exchange kinetics, which has been relatively well-studied.[47−49] Time-resolved small-angle neutron scattering (SANS) studies by Lund et al.[50,51] recently revealed that the equilibrium exchange kinetics exhibits a logarithmic time dependence. However, their experimental design was such that kinetic information during the first 1−2 min was missing. For simplicity, double-exponential functions were still employed to analyze the kinetic curves in this study.

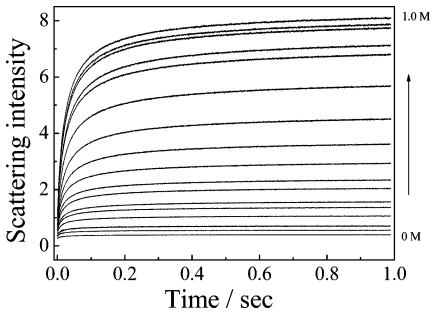

Figure 4. Time dependence of the scattering light intensity at various final NaCl concentrations caused by a pH jump from 4 to 12. The final copolymer concentration is fixed at 1.0 g/L.

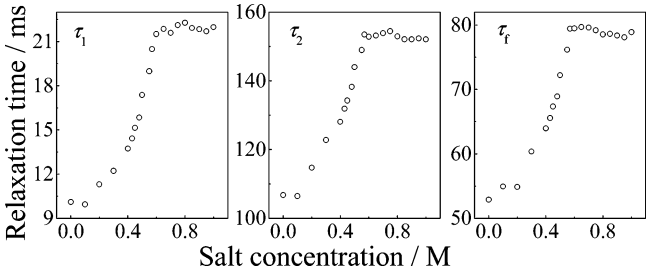

Figure 5. Double-exponential fits obtained for micelle formation at various NaCl concentrations. The experimental conditions are the same as those described in Figure 4.

For the pH jump from 4 to 12 at a copolymer concentration of 1.0 g/L in the presence of 1.0 M NaCl, the relaxation times τ_1 and τ_2 were calculated to be 22 and 150 ms, respectively. Thus, τ_f is calculated to be 78 ms from eq 3. As a comparison, the data obtained for the same copolymer concentration in salt-free solution were $\tau_1 = 10$ ms, $\tau_2 = 106$ ms, and $\tau_f = 43$ ms. Hence, we conclude that the kinetics of micellization is significantly slower in the presence of salt.

We further studied the salt concentration dependence of the characteristic relaxation times for micellization. Figure 4 shows the time dependence of the scattering light intensity at various final NaCl concentrations during micelle formation at a fixed copolymer concentration. The stopped-flow apparatus used in this study has a dead time of ~2−3 ms. All the relaxation curves shown in Figure 4 overlap at the starting point, i.e., 2−3 ms after mixing. This indicates that no major kinetic events occur within the stopped-flow dead time upon variation of the salt concentrations.

The results obtained from double-exponential fitting of the kinetic curves in Figure 4 are shown in Figure 5. The characteristic relaxation time constants τ_1, τ_2, and τ_f clearly increase with increasing NaCl concentration initially and then level off at higher salt concentrations (>0.5 M). This indicates that added salt can dramatically retard the micellization kinetics. This may be simply because the presence of salt leads to larger micelle aggregation numbers, thus requiring longer time scales, as predicted by Dormidontova et al.[33] Moreover, the presence of salt leads to micelles with more compact cores and partially dehydrated coronas. Thus, the micelle formation/breakup process will be inevitably slower, regardless of whether it proceeds via the unimer insertion/expulsion or micelle fusion/fission mechanism.

Copolymer Concentration Dependence of Micellization Kinetics. Furthermore, we studied the copolymer concentration dependence of τ_1 and τ_2 for a pH jump from 4 to 12 in the presence of 1.0 M NaCl. Results shown in Figure 2 have already

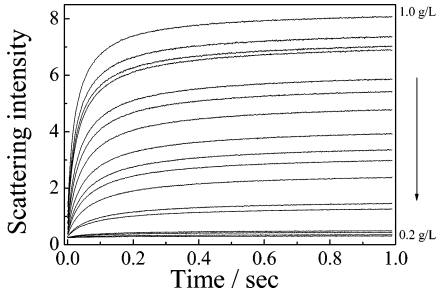

Figure 6. Time dependence of the scattering light intensity at various final copolymer concentrations caused by a pH jump from 4 to 12 in the presence of 1.0 M NaCl.

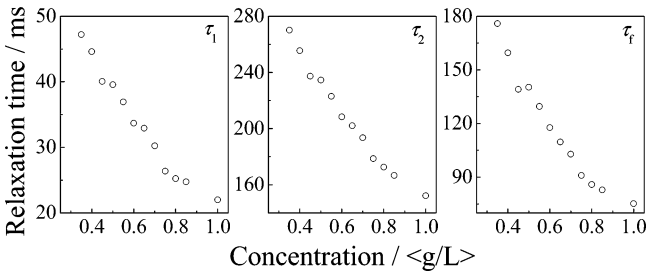

Figure 7. Double-exponential fits obtained for micellization at various copolymer concentrations in the presence of 1.0 M NaCl. The experimental conditions are the same as those described in Figure 6.

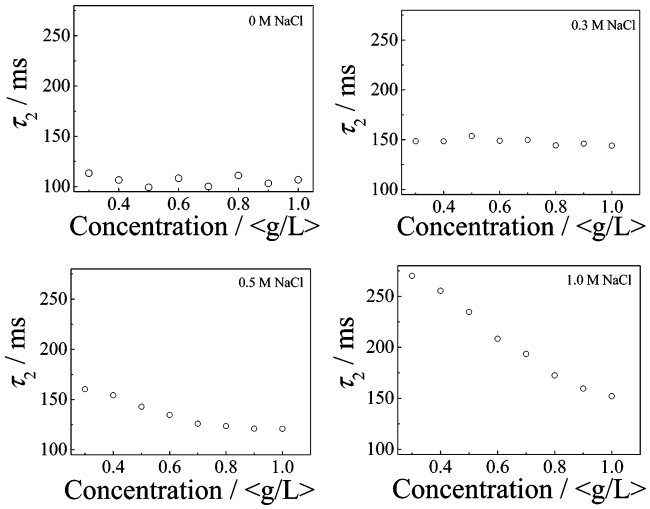

Figure 8. Concentration dependence for the relaxation time constant corresponding to the slow process (τ_2) in the presence of added NaCl.

revealed that variation of copolymer concentration did not affect either the micelle size or micelle density. The dynamic curves at different copolymer concentrations and in the presence of 1.0 M NaCl are shown in Figure 6. If the final copolymer concentration is below 0.2 g/L, which is close to the critical micellization concentration (cmc), we do not observe any relaxation process since the kinetic curves remain linear. Above a copolymer concentration of 0.2 g/L, relaxation processes with positive amplitudes are typically observed.

Similarly, the relaxation curves shown in Figure 6 can be well fitted with a double-exponential function. The values of τ_1, τ_2, and τ_f (calculated using eq 3) are shown in Figure 7. For the fast process, τ_1 ranges from 22 to 48 ms, which decreases with increasing copolymer concentration. For the slow process, τ_2 ranges from 150 to 270 ms and also decreases at higher copolymer concentrations.

τ_1 is associated with the rapid association of unimers into large numbers of small micelles and the formation of quasi-

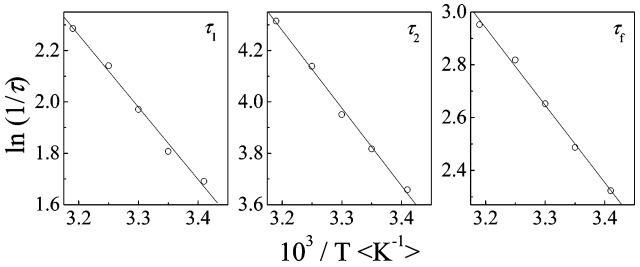

Figure 9. Arrhenius plots obtained for τ_1, τ_2, and τ_f for a pH jump from 4 to 12 in the presence of 1.0 M NaCl. The final copolymer concentration is fixed at 1.0 g/L.

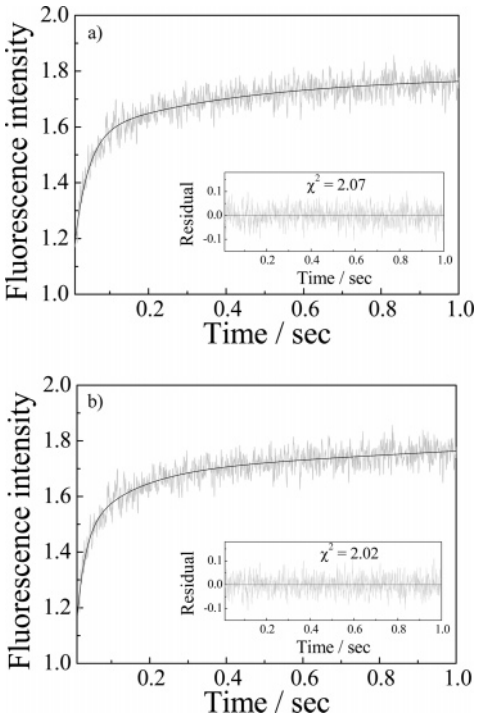

Figure 10. Time dependence of the fluorescence intensity (I_m, 370 nm) for a pyrene probe. Curves are fitted by (a) single- and (b) double-exponential functions. The pyrene concentration is 10^{-6} M, and the copolymer concentration is 1.0 g/L in the presence of 1.0 M NaCl.

equilibrium micelles. A schematic illustration is shown in Scheme 1. For a pH jump from 4 to 12, unimers quickly aggregate into small micelles, and the driving force is the large excess of unimers. The formation of such small micelles with low aggregation numbers involves little or no stretching of the solvated PGMA and PDMA blocks.

The growth of small micelles into quasi-equilibrium micelles can proceed by either the unimer insertion/expulsion mechanism[31] or the fusion/fission mechanism.[26] Previously, we postulated that the latter mechanism dominates during the growth of small micelles into quasi-equilibrium micelles, as predicted by Dormidontova et al.[33] Micelle fusion proceeds via intermicelle collisions; the two micelle cores must come into contact to form quasi-equilibrium micelles. There is only a low-energy barrier for fusion between small micelles because the PGMA and PDMA blocks are less stretched for low aggregation numbers. Thus, the observed concentration dependence of τ_1 is readily understood if the growth of small micelles into quasi-equilibrium micelles occurs via a micelle fusion/fission mechanism.

At the end of the initial fast process, the quasi-equilibrium micelles have much larger micelle aggregation numbers than those of the original small micelles. The coronal chains will

Scheme 1. Schematic Illustration of Micelle Growth via the Unimer Insertion/Expulsion and Micelle Fusion/Fission Mechanisms

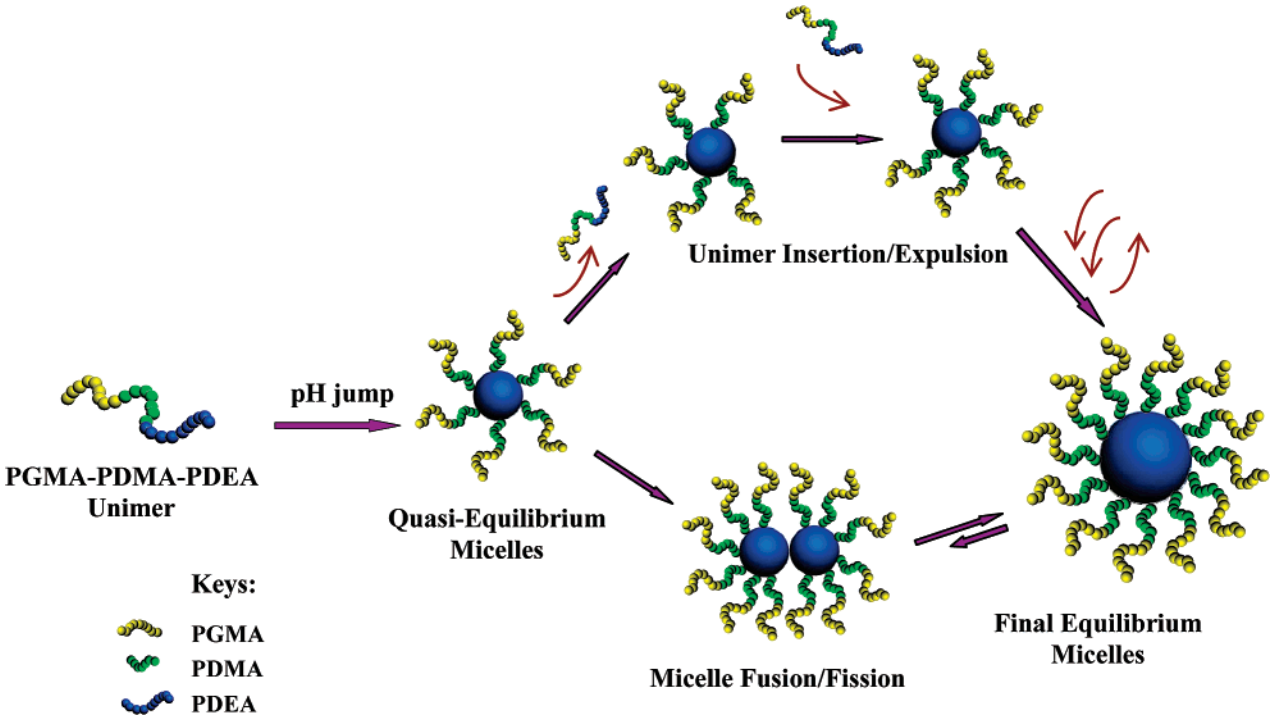

become more stretched; hence, micelle growth via the micelle fusion/fission mechanism encounters higher energy barriers, leading to a slower growth rate. This retardation leads to the second slow process, i.e., micelle formation/breakup. In our previous studies of the micellization kinetics of PGMA-*b*-PDMA-*b*-PDEA triblock copolymer in the absence of salt, τ_2 was almost independent of copolymer concentration.[40] We postulated that micelle formation/breakup proceeds via unimer insertion/expulsion. In contrast, τ_2 decreases with increasing copolymer concentration in the presence of 1.0 M NaCl (Figure 7). This strongly suggests that the slow process involves micelle fusion/fission (Scheme 1). Dormidontova et al.[33] predicted that the characteristic time step for micelle fusion/fission in dilute solution is inversely proportional to the copolymer concentration.

Figure 8 shows the effect of added salt on the characteristic relaxation time constant of the slow process (τ_2) as a function of copolymer concentration. In the presence of 0 and 0.3 M NaCl, τ_2 has no discernible copolymer concentration dependence. However, in the presence of 0.5 M NaCl, τ_2 begins to decrease with copolymer concentration, similar to the data obtained for 1.0 M NaCl. Thus, 0.5 M NaCl corresponds approximately to the inflection point, where the micelle formation/breakup mechanism changes from unimer insertion/expulsion to micelle fusion/fission. It is noteworthy that this critical concentration (0.5 M NaCl) also corresponds to that where there is no further change in τ_2 with increasing salt concentration (Figure 5, Scheme 1).

Increasing ionic strength may exert several effects on the micellization process. First, the micelle cores become more compact in the presence of salt, so it is reasonable to suppose that unimer expulsion will encounter higher energy barriers compared to that obtained with salt-free solutions. Thus, the driving force for the unimer insertion/expulsion mechanism, which is the excess unimer generated by dissociation of some of the quasi-equilibrium micelles, is reduced. Second, the PGMA and PDMA blocks become partially dehydrated by the added salt; thus, the less stretched coronal chains will lead to reduced steric repulsion between micelles, thus increasing the probability of micelle fusion. Finally, in the presence of added salt, cmc values should decrease due to the reduced hydrophilic character of all three blocks and the low unimer concentration will make the unimer insertion/expulsion mechanism less favorable.

Figure 9 shows the temperature dependence of τ_1, τ_2, and τ_f for the micellization that results from a pH jump from 4 to 12 in the presence of 0.1 M NaCl. An inverse temperature dependence was expected for τ_1, τ_2, and τ_f, as observed for conventional surfactants. The Arrhenius plots in Figure 9 indicate activation energies of 24.9, 23.2, and 24.3 kJ mol^{-1} for the processes associated with τ_1, τ_2, and τ_f, respectively, which are systematically higher than the corresponding activation energies calculated for salt-free copolymer micelle solutions. This indicates that added salt leads to a significant increase in the energy barrier for both processes, leading directly to the slower relaxation kinetics observed in the current study.

Stopped-Flow Fluorescence Studies. Changes in pyrene fluorescence are frequently used to monitor the onset of micellization for various amphiphilic block copolymers.[52] The so-called "monomer" fluorescence is mainly determined by the local concentration of pyrene within the hydrophobic micelle cores.

All copolymer solutions prior to stopped-flow mixing were solubilized with pyrene. During micelle formation, this probe was expected to diffuse into the hydrophobic micelle core, leading to a local increase in pyrene concentration within the micelles. Figure 10 shows the time dependence of the monomer fluorescence intensity (I_m, 370 nm) of pyrene during micellization in the presence of 1.0 M NaCl, together with the single- and double-exponential fitting results. On the basis of eq 1, the calculated χ^2 error values are 2.07 and 2.02 for the single- and double-exponential fitting, respectively. As the χ^2 error value of the double-exponential fitting does not improve appreciably as compared to that of the single-exponential fitting, we conclud that dynamic trace of fluorescence intensities can be well-fitted by a single-exponential function.

Liu et al.[53] reported the kinetics of chain exchange after mixing two types of PS-*b*-PCEMA micelles, one containing

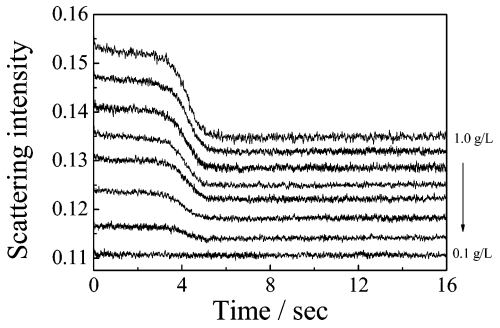

Figure 11. Time dependence of the scattering light intensity recorded during micelle dissociation for a pH jump from 12 to 4 in the presence of 1.0 M NaCl at various final copolymer concentrations.

pyrene tags and the other containing no pyrene. The recorded time dependence curve of monomer fluorescence intensity was fitted by double-exponential functions. It should be noted that the process they investigated should be ascribed to the equilibrium chain exchange kinetics, which is different from the micelle formation process in the current case. Moreover, they do not ascribe the detected two relaxation times with any specific physical processes.

The single-exponential fitting gives a characteristic relaxation time constant τ_{py} of 55 ms. This stopped-flow fluorescence value agrees quite well with τ_f, which is the characteristic relaxation time (based on eq 3), obtained by stopped-flow light scattering for the overall micellization process.

During the initial fast process, unimers rapidly associate into small transient micelles, which then further grow into quasi-equilibrium micelles. The subsequent slow process is associated with an increase in the micelle aggregation number and a reduction in the number density of micelles. From Figure 10, the monomer fluorescence intensity initially increased rapidly, before becoming constant. Since there is only one characteristic time constant, we deduce that both the initially formed small micelles and quasi-equilibrium micelles do not possess well-defined core−shell nanostructures and that in both cases the micelle cores are less dehydrated compared to the final equilibrium micelles.

Micellization Dissociation Kinetics. We have also studied the kinetics for the micelle-to-unimer transition that occurs for a pH jump from 12 to 4 in the presence of 1.0 M NaCl. Relaxation curves for this dissociation process at various copolymer concentrations are shown in Figure 11, which reveals an intriguing two-stage relaxation process. Within the stopped-flow dead time (2−3 ms), the scattering intensities decrease dramatically compared to the original intensities recorded at pH 12. However, after a delay time of ∼3−4 s, a distinct second stage for the reduction in light scattering intensity was clearly discernible, especially at higher copolymer concentration. Currently, we cannot explain this two-stage dissociation process. However, it is noteworthy that this behavior was not observed with salt-free copolymer micelles. This underlines the profound influence that added salt can have on the dynamics of micellization and dissociation for such pH-responsive block copolymers.

Conclusions

Stopped-flow light scattering and fluorescence techniques have been used to investigate the effect of added salt on the pH-induced micellization kinetics of a PGMA-*b*-DMA-*b*-PDEA triblock copolymer. For micelle formation in the presence or absence of salt, all relaxation curves recorded by stopped-flow light scattering can be well-fitted using a double-exponential function, leading to a fast relaxation time constant (τ_1) and a slow relaxation time constant (τ_2). The first parameter is associated with the formation of quasi-equilibrium micelles, while the latter is associated with micelle formation−breakup on approaching the final equilibrium state. Both time constants are dramatically reduced for lower concentrations of added salt and then level off at higher salt concentrations (>0.5 M NaCl). The copolymer concentration dependence of τ_2 revealed that the micelle formation/breakup mechanism changes from unimer insertion/expulsion in the absence of salt to micelle fusion/fission in the presence of high salt (>0.5 M NaCl). This is due to the added salt causing both partial dehydration of the PGMA and PDMA blocks and also more compact PDEA cores. Stopped-flow fluorescence relaxation curves obtained using a pyrene probe can be well-fitted with a single-exponential function, and the characteristic relaxation time (τ_{py}) agreed well with τ_f, which is the relaxation time for the overall micellization process as determined by stopped-flow light scattering. This indicates that the initially formed quasi-equilibrium micelles do not possess a well-defined core−shell structure and the micelle cores are not fully dehydrated. Compared to our previous study conducted in the absence of added salt, the pH-induced micelle dissociation kinetics in the presence of salt reveals a drastically different two-stage process, with a delay time of a few seconds between the two stages.

Acknowledgment. This work was financially supported by an Outstanding Youth Fund (50425310) and research grants (20534020, 20674079) from the National Natural Scientific Foundation of China (NNSFC) and the "Bai Ren" Project of the Chinese Academy of Sciences. S.P.A. is the recipient of a five-year Royal Society-Wolfson Research Merit Award.

References and Notes

(1) Hamley, I. W. *The Physics of Block Copolymers*; Oxford University Press: Oxford, 1998.
(2) Fustin, C. A.; Abetz, V.; Gohy, J. F. *Eur. Phys. J. E* **2005**, *16*, 291−302.
(3) Gohy, J. F. *Adv. Polym. Sci.* **2005**, *190*, 65−136.
(4) Hadjichristidis, N.; Iatrou, H.; Pitsikalis, M.; Pispas, S.; Avgeropoulos, A. *Prog. Polym. Sci.* **2005**, *30*, 725−782.
(5) Riess, G. *Prog. Polym. Sci.* **2003**, *28*, 1107−1170.
(6) Rodriguez-Hernandez, J.; Checot, F.; Gnanou, Y.; Lecommandoux, S. *Prog. Polym. Sci.* **2005**, *30*, 691−724.
(7) Colfen, H. *Macromol. Rapid Commun.* **2001**, *22*, 219−252.
(8) Rodriguez-Hernandez, J.; Lecommandoux, S. *J. Am. Chem. Soc.* **2005**, *127*, 2026−2027.
(9) Arotcarena, M.; Heise, B.; Ishaya, S.; Laschewsky, A. *J. Am. Chem. Soc.* **2002**, *124*, 3787−3793.
(10) Virtanen, J.; Arotcarena, M.; Heise, B.; Ishaya, S.; Laschewsky, A.; Tenhu, H. *Langmuir* **2002**, *18*, 5360−5365.
(11) Andre, X.; Zhang, M. F.; Muller, A. H. E. *Macromol. Rapid Commun.* **2005**, *26*, 558−563.
(12) Alarcon, C. D. H.; Pennadam, S.; Alexander, C. *Chem. Soc. Rev.* **2005**, *34*, 276−285.
(13) Butun, V.; Liu, S.; Weaver, J. V. M.; Bories-Azeau, X.; Cai, Y.; Armes, S. P. *React. Funct. Polym.* **2006**, *66*, 157−165.
(14) Liu, S. Y.; Armes, S. P. *Angew. Chem., Int. Ed.* **2002**, *41*, 1413−1416.
(15) Bo, Q.; Zhao, Y. *J. Polym. Sci., Part A: Polym. Chem.* **2006**, *44*, 1734−1744.
(16) Li, Y. T.; Armes, S. P.; Jin, X. P.; Zhu, S. P. *Macromolecules* **2003**, *36*, 8268−8275.
(17) Ma, Y. H.; Tang, Y. Q.; Billingham, N. C.; Armes, S. P.; Lewis, A. L.; Lloyd, A. W.; Salvage, J. P. *Macromolecules* **2003**, *36*, 3475−3484.
(18) Mountrichas, G.; Pispas, S. *Macromolecules* **2006**, *39*, 4767−4774.
(19) Pispas, S. *J. Polym. Sci., Part A: Polym. Chem.* **2006**, *44*, 606−613.
(20) Vamvakaki, M.; Palioura, D.; Spyros, A.; Armes, S. P.; Anastasiadis, S. H. *Macromolecules* **2006**, *39*, 5106−5112.
(21) Vandermeulen, G. W. M.; Tziatzios, C.; Duncan, R.; Klok, H. A. *Macromolecules* **2005**, *38*, 761−769.

(22) Zhang, W. Q.; Shi, L. Q.; Ma, R. J.; An, Y. L.; Xu, Y. L.; Wu, K. *Macromolecules* **2005**, *38*, 8850−8852.
(23) Aniansson, E. A. G.; Wall, S. N. *J. Phys. Chem.* **1974**, *78*, 1024−1030.
(24) Aniansson, E. A. G.; Wall, S. N. *J. Phys. Chem.* **1975**, *79*, 857−858.
(25) Aniansson, E. A. G.; Wall, S. N.; Almgren, M.; Hoffmann, H.; Kielmann, I.; Ulbricht, W.; Zana, R.; Lang, J.; Tondre, C. *J. Phys. Chem.* **1976**, *80*, 905−922.
(26) Kahlweit, M. *J. Colloid Interface Sci.* **1982**, *90*, 92−99.
(27) Lessner, E.; Teubner, M.; Kahlweit, M. *J. Phys. Chem.* **1981**, *85*, 1529−1536.
(28) Rharbi, Y.; Winnik, M. A. *Adv. Colloid Interface Sci.* **2001**, *89*, 25−46.
(29) Patist, A.; Kanicky, J. R.; Shukla, P. K.; Shah, D. O. *J. Colloid Interface Sci.* **2002**, *245*, 1−15.
(30) Noskov, B. A. *Adv. Colloid Interface Sci.* **2002**, *95*, 237−293.
(31) Halperin, A.; Alexander, S. *Macromolecules* **1989**, *22*, 2403−2412.
(32) Wang, Y. M.; Mattice, W. L.; Napper, D. H. *Langmuir* **1993**, *9*, 66−70.
(33) Dormidontova, E. E. *Macromolecules* **1999**, *32*, 7630−7644.
(34) Nyrkova, I. A.; Semenov, A. N. *Macromol. Theory Simul.* **2005**, *14*, 569−585.
(35) Nyrkova, I. A.; Semenov, A. N. *Faraday Discuss.* **2005**, *128*, 113−127.
(36) Honda, C.; Hasegawa, Y.; Hirunuma, R.; Nose, T. *Macromolecules* **1994**, *27*, 7660−7668.
(37) Honda, C.; Abe, Y.; Nose, T. *Macromolecules* **1996**, *29*, 6778−6785.
(38) Iyama, K.; Nose, T. *Macromolecules* **1998**, *31*, 7356−7364.
(39) Iyama, K.; Nose, T. *Kobunshi Ronbunshu* **2001**, *58*, 273−278.
(40) Zhu, Z. Y.; Armes, S. P.; Liu, S. Y. *Macromolecules* **2005**, *38*, 9803−9812.
(41) He, E.; Ravi, P.; Tam, K. C. *Langmuir* **2007**, *23*, 2382−2388.
(42) Jain, N. J.; Aswal, V. K.; Goyal, P. S.; Bahadur, P. *J. Phys. Chem. B* **1998**, *102*, 8452−8458.
(43) Perreur, C.; Habas, J. P.; Lapp, A.; Peyrelasse, J. *Polymer* **2006**, *47*, 841−848.
(44) Ma, J. H.; Guo, C.; Tang, Y. L.; Wang, J.; Zheng, L.; Liang, X. F.; Shen, S.; Liu, H. Z. *Langmuir* **2007**, *23*, 3075−3083.
(45) Sedlak, M. *Surfactant Science Series*; Redeva, T., Ed.; Marcel Dekker: New York, 2001.
(46) Kositza, M. J.; Bohne, C.; Hatton, T. A.; Holzwarth, J. F. *Prog. Colloid Polym. Sci.* **1999**, *112*, 146−151.
(47) Haliloglu, T.; Bahar, I.; Erman, B.; Mattice, W. L. *Macromolecules* **1996**, *29*, 4764−4771.
(48) Smith, C. K.; Liu, G. J. *Macromolecules* **1996**, *29*, 2060−2067.
(49) Wang, Y. M.; Kausch, C. M.; Chun, M. S.; Quirk, R. P.; Mattice, W. L. *Macromolecules* **1995**, *28*, 904−911.
(50) Lund, R.; Willner, L.; Richter, D.; Dormidontova, E. E. *Macromolecules* **2006**, *39*, 4566−4575.
(51) Lund, R.; Willner, L.; Stellbrink, J.; Lindner, P.; Richter, D. *Phys. Rev. Lett.* **2006**, *96*, 068302.
(52) Briks, J. B. *Photophysics of Aromatic Molecules*; Wiley: New York, 1970.
(53) Underhill, R. S.; Ding, J. F.; Birss, V. I.; Liu, G. J. *Macromolecules* **1997**, *30*, 8298−8303.

MA070978H